



Nonlinear Inelastic Nonuniform Torsion of Bars including the Secondary Torsional Moment Deformation Effect

V.J. Tsipiras and E.J. Sapountzakis
School of Civil Engineering
National Technical University, Athens, Greece

Abstract

In this paper a boundary element method (BEM) is developed for the inelastic nonuniform torsional problem of simply or multiply connected prismatic bars of arbitrarily shaped doubly symmetric cross section, taking into account the effects of geometrical nonlinearity and secondary torsional moment deformation. The bar is subjected to arbitrarily distributed or concentrated axial and torsional loading along its length, while its edges are subjected to the most general axial and torsional boundary conditions. Inelastic redistribution is modelled through a distributed plasticity model while the transverse displacement components are expressed so as to be valid for large twisting rotations. A torsional shear correction factor (determined through an energy approach) is employed to model secondary torsional moment deformation effects. A modified Powell hybrid algorithm is adopted within an incremental formulation to resolve the elastic and plastic parts of stress resultants. Three boundary value problems are formulated and solved employing the boundary element method.

Keywords: nonuniform torsion, inelastic torsion, nonlinear torsion, Wagner strain, warping, secondary torsional moment deformation effect, torsional shear correction factor, warping shear stresses, distributed plasticity, boundary element method, bar.

1 Introduction

In engineering practice we often come across the analysis of members of structures subjected to twisting moments. Curved bridges, ribbed plates subjected to eccentric loading or columns laid out irregularly in the interior of a plate due to functional requirements are most common examples. Analyses of these structures based on elastic constitutive equations are most likely to lead to extremely conservative designs not only due to significant difference between first yield in a cross section and full plasticity but also due to the unaccounted for yet significant reserves of

strength that are enabled only after inelastic redistribution along members takes place. Moreover, inelastic deformations are often associated with significant material stiffness degradation, usually resulting in geometrically nonlinear effects in structures made of ductile materials. These effects also occur in frequently employed members of low torsional stiffness. Thus, both material and geometrical nonlinearities are important for investigating the ultimate strength of a bar that resists torsional loading, while distributed plasticity models are acknowledged in the literature [1] to capture more rigorously material nonlinearities than cross sectional stress resultant approaches or lumped plasticity idealizations.

When an elastic bar is subjected to uniform torque arising from two concentrated torsional moments at its ends while the warping of the cross section is not restrained, the angle of twist per unit length remains constant along the bar. Under these conditions, the bar is leded to uniform torsion and the well known primary (St. Venant) shear stress distribution arises forming the primary torsional moment stress resultant. When arbitrary torsional boundary conditions are applied either at the edges or at any other interior point of a bar due to construction requirements, this bar under the action of general twisting loading is leded to nonuniform torsion and additional normal and secondary (warping) shear stresses arise [2], forming the warping moment and secondary torsional moment stress resultants, respectively. In order to include warping shear stresses in the global equilibrium of the bar, that is to account for the secondary torsional moment deformation effect (STMDE), an additional kinematical component (along with the angle of twist) is generally required (see for example [3-4]), increasing the difficulty of the problem at hand. The problem becomes more complicated when finite twisting rotations are considered (geometrical nonlinearity) due to the fact that axial and torsional kinematical components and the associated equilibrium equations are coupled [5]. If inelastic effects are considered as well, especially through distributed plasticity formulations, the nonlinear inelastic nonuniform torsional problem including STMDE requires a much more rigorous analysis.

As early as 1954, Benscoter analyzed bars of multicell cross sections taking into account STMDE. The STMDE at the elastic geometrically linear regime has been shown in the literature to be significant, especially on closed shaped section bars. In order to satisfy local equilibrium considerations, a torsional shear correction factor is required at the global level to correct the secondary torsion constant [4] along with a suitable warping shear stress distribution at the local level [3-4].

During the past years, the nonlinear inelastic nonuniform torsional analysis of bars taking into account [6] or ignoring [7] STMDE has received a good amount of attention in the literature. The interested reader may study the literature surveys of [8-9]. Most of the relevant contributions are restricted to cross sections of special geometry while to the authors' knowledge none research effort includes the torsional shear correction factor in the analysis of STMDE. This has been achieved in the recent contribution of Tsipiras and Sapountzakis [9] which is however restricted to the geometrically linear regime. Moreover, alternative methodologies that may rigorously capture several effects including STMDE without the aforementioned factor have also been recently presented (see the relevant references cited in [9]), however a multitude of local or global warping functions are required. Finally, it is

worth here noting that to the authors' knowledge the BEM has not yet been employed to the nonlinear inelastic nonuniform torsional problem of bars. The essential features and novel aspects of the present formulation compared with previous ones are summarized as follows.

- i. For the first time in the literature, STMDE is taken into account to the problem at hand and its influence is quantified. Evaluation of St. Venant and warping shear stresses is based on the solution of boundary value problems formulated by exploiting local equilibrium considerations at the elastic geometrically linear regime. A torsional shear correction factor, determined through an energy approach, is also employed to capture STMDE more rigorously.
- ii. Large twisting rotations are taken into account that is the strain-displacement relationships contain higher order displacement terms.
- iii. The cross section is an arbitrarily shaped thin- or thick-walled doubly symmetric one. The formulation does not stand on the assumptions of a thin-walled structure and therefore the cross section's rigidities are evaluated "exactly" in a numerical sense.
- iv. An incremental - iterative solution strategy is adopted to resolve the elastic and plastic parts of the stress resultants. The system of discretized global equilibrium equations is expressed without explicitly deriving its incremental form which is lengthier due to terms associated with geometrical nonlinearity. Integration of the inelastic rate equations is performed at each monitoring station with an efficient iterative process.
- v. The developed procedure retains most of the advantages of a BEM solution over a pure domain discretization method, although it requires domain discretization to the longitudinal problem, exhibiting the following features.
 - Shear locking is alleviated by employing the same order of approximation for both the total and the primary part of the angle of twist per unit length.
 - Membrane locking is alleviated by exploiting the boundary integral representation of the "average" axial displacement per unit length.
 - Cross sectional discretization is employed exclusively for numerical integration of domain integrals.
 - Finite differences and differentiation of shape functions are not required.

2 Statement of the problem

2.1 Displacements, strains, stresses

Consider a prismatic bar of length l (Figure 1) with an arbitrarily shaped doubly symmetric constant cross section, occupying the two dimensional multiply connected region Ω of the y, z plane bounded by the Γ_j ($j = 1, 2, \dots, K$) boundary curves, which are piecewise smooth, i.e. they may have a finite number of corners. In Figure 1a S_{yz} is the coordinate system through the cross section's shear center. The normal stress-strain relationship for the material is assumed to be elastic-plastic-strain hardening with initial modulus of elasticity E , shear modulus G , post-yield

modulus of elasticity E_t and initial yield stress σ_{Y0} . The bar is subjected to the combined action of arbitrarily distributed or concentrated axial load $n(x)$ and twisting $m_t = m_t(x)$ and warping $m_w = m_w(x)$ moments acting in the x direction (Figure 1b).

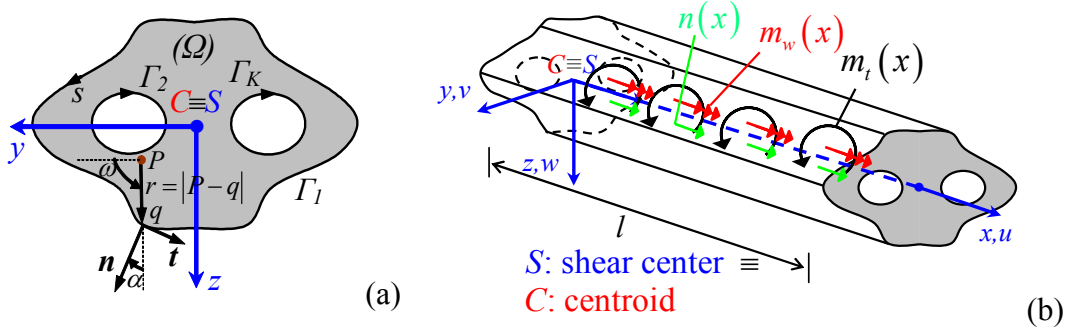


Figure 1: Prismatic bar of an arbitrarily shaped doubly symmetric cross section occupying region Ω (a) subjected to axial and torsional loading (b).

Under the aforementioned loading, the displacement field of the bar taking into account secondary torsional moment deformation effects and large twisting rotations is assumed to be given as

$$u(x, y, z) = u_m(x) + \left(\theta_x^P(x)\right)' \phi_S^P(y, z) \quad (1a)$$

$$v(x, y, z) = -z \sin \theta_x(x) - y(1 - \cos \theta_x(x)) \quad (1b)$$

$$w(x, y, z) = y \sin \theta_x(x) - z(1 - \cos \theta_x(x)) \quad (1c)$$

where u, v, w are the axial and transverse bar displacement components with respect to the Syz system of axes; θ_x is the (total) angle of twist; $\left(\theta_x^P\right)'$ is the primary angle of twist per unit length [4] which is in general not equal to the angle of twist per unit length θ_x' ; u_m is an ‘‘average’’ axial displacement of the bar’s cross section [10]; ϕ_S^P is the primary warping function with respect to the shear center S [2].

Substituting Equations (1) in the nonlinear strain-displacement relations of the Green strain tensor and exploiting the assumptions of moderate displacements $((\partial u/\partial x)^2 \ll \partial u/\partial x, (\partial u/\partial x)(\partial u/\partial y) \ll \partial v/\partial x + \partial u/\partial y, (\partial u/\partial x)(\partial u/\partial z) \ll \partial w/\partial x + \partial u/\partial z)$ [11], the nonvanishing compatible (total) strain resultants are obtained as

$$\varepsilon_{xx} = u_m' + \left(\theta_x^P\right)'' \phi_S^P + \frac{1}{2}(y^2 + z^2)(\theta_x')^2 \quad (2a)$$

$$\gamma_{xy} = \underbrace{\theta'_x \left(\frac{\partial \phi_S^P}{\partial y} - z \right)}_{\text{primary}} + \underbrace{\left((\theta_x^P)' - \theta'_x \right) \frac{\partial \phi_S^P}{\partial y}}_{\text{secondary}} \quad (2b)$$

$$\gamma_{xz} = \underbrace{\theta'_x \left(\frac{\partial \phi_S^P}{\partial z} + y \right)}_{\text{primary}} + \underbrace{\left((\theta_x^P)' - \theta'_x \right) \frac{\partial \phi_S^P}{\partial z}}_{\text{secondary}} \quad (2c)$$

where in Equations (2b,c), the first terms correspond to St. Venant shear strains ($\gamma_{xy}^P, \gamma_{xz}^P$) and the last terms to warping ones ($\gamma_{xy}^S, \gamma_{xz}^S$), while the nonlinear term in the right hand side of Equation (2a) is often characterized as the ‘‘Wagner strain’’ [7]. In order to formulate global equilibrium equations at the elastic geometrically linear regime that include torsional shear correction factor (see [4, 9]), the above relations are proposed to be corrected as

$$\varepsilon_{xx} = u'_m + (\theta_x^P)'' \phi_S^P + \frac{1}{2}(y^2 + z^2)(\theta'_x)^2 \quad (3a)$$

$$\gamma_{xy} = \underbrace{\theta'_x \left(\frac{\partial \phi_S^P}{\partial y} - z \right)}_{\text{primary}} + \underbrace{\left((\theta_x^P)' - \theta'_x \right) \sqrt{k_x} \frac{\partial \phi_S^P}{\partial y}}_{\text{secondary}} \quad (3b)$$

$$\gamma_{xz} = \underbrace{\theta'_x \left(\frac{\partial \phi_S^P}{\partial z} + y \right)}_{\text{primary}} + \underbrace{\left((\theta_x^P)' - \theta'_x \right) \sqrt{k_x} \frac{\partial \phi_S^P}{\partial z}}_{\text{secondary}} \quad (3c)$$

where k_x is the torsional shear correction factor [4, 9]. The elastic geometrically linear shear stress distribution arising from Equations (3) yields equilibrium equations that are corrected at the global level, however it still violates the longitudinal local equilibrium equation [9]. Thus a two dimensional secondary warping function $\phi_S^S(y, z)$ [9] is introduced as

$$\varepsilon_{xx} = u'_m + (\theta_x^P)'' \phi_S^P + \frac{1}{2}(y^2 + z^2)(\theta'_x)^2 \quad (4a)$$

$$\gamma_{xy} = \underbrace{\theta'_x \left(\frac{\partial \phi_S^P}{\partial y} - z \right)}_{\text{primary}} + \underbrace{\left((\theta_x^P)' - \theta'_x \right) \left(-\frac{I_t^S}{C_S} \right) \frac{\partial \phi_S^S}{\partial y}}_{\text{secondary}} \quad (4b)$$

$$\gamma_{xz} = \underbrace{\theta'_x \left(\frac{\partial \phi_S^P}{\partial z} + y \right)}_{\text{primary}} + \underbrace{\left((\theta_x^P)' - \theta'_x \right) \left(-\frac{I_t^S}{C_S} \right) \frac{\partial \phi_S^S}{\partial z}}_{\text{secondary}} \quad (4c)$$

where I_t^S and C_S are the secondary torsion constant and warping constant, respectively [4, 9] (see Equations (13d,f)). Both the primary and the secondary warping functions are determined by formulating boundary value problems based on the exploitation of the longitudinal local equilibrium equation and the associated boundary condition [4, 9]. Formulation arising from Equations (2) corresponds to the use of constant strain distribution in the nonlinear Timoshenko beam theory without employing a shear correction factor, while the ones arising from Equations (3) and (4) correspond to the use of constant and parabolic strain distribution in the same theory, respectively.

Considering strains to be small, employing the second Piola – Kirchhoff stress tensor [12], assuming an isotropic and homogeneous material without exhibiting any damage during its plastification and neglecting the S_{yy} , S_{zz} , S_{yz} components, the stress rates are defined in terms of the strain ones as

$$dS_{xx} = Ed\varepsilon_{xx}^{el} \quad dS_{xy} = Gd\gamma_{xy}^{el} \quad dS_{xz} = Gd\gamma_{xz}^{el} \quad (5a,b,c)$$

where $d(\cdot)$ denotes infinitesimal incremental quantities over time (rates) and the superscript *el* denotes the elastic part of the strain components.

As long as the material remains elastic or elastic unloading occurs, that is

$$\left\{ d\varepsilon_{xx} \quad d\gamma_{xy} \quad d\gamma_{xz} \right\}^T = \left\{ d\varepsilon_{xx}^{el} \quad d\gamma_{xy}^{el} \quad d\gamma_{xz}^{el} \right\}^T \quad (6)$$

the stress rates are given with respect to the total strain ones by combining Equations (5), (6). If plastic flow occurs then

$$\left\{ d\varepsilon_{xx} \quad d\gamma_{xy} \quad d\gamma_{xz} \right\}^T = \left\{ d\varepsilon_{xx}^{el} \quad d\gamma_{xy}^{el} \quad d\gamma_{xz}^{el} \right\}^T + \left\{ d\varepsilon_{xx}^{pl} \quad d\gamma_{xy}^{pl} \quad d\gamma_{xz}^{pl} \right\}^T \quad (7)$$

where the superscript *pl* denotes the plastic part of the strain components. The stress rates are given with respect to the total and plastic strain ones through Equations (5), (7) as

$$dS_{xx} = Ed\varepsilon_{xx} - Ed\varepsilon_{xx}^{pl} \quad dS_{xy} = Gd\gamma_{xy} - Gd\gamma_{xy}^{pl} \quad dS_{xz} = Gd\gamma_{xz} - Gd\gamma_{xz}^{pl} \quad (8a,b,c)$$

A Von Mises yield criterion, an associated flow rule and an isotropic hardening rule for the material are considered [12], permitting the determination of the plastic strain components. The yield condition is described with the expression

$$f = \sqrt{S_{xx}^2 + 3(S_{xy}^2 + S_{xz}^2)} - \sigma_Y(\varepsilon_{eq}^{pl}) = 0 \quad (9)$$

where σ_Y is the yield stress of the material and ε_{eq}^{pl} is the equivalent plastic strain, the rate of which is defined in [12].

2.2 Equations of global equilibrium

To establish global equilibrium equations, the principle of virtual work under a Total Lagrangian formulation neglecting body forces is employed

$$\int_V (S_{xx}\delta\varepsilon_{xx} + S_{xy}\delta\gamma_{xy} + S_{xz}\delta\gamma_{xz}) dV = \int_F (t_x\delta u + t_y\delta v + t_z\delta w) dF \quad (10)$$

where $\delta(\cdot)$ denotes virtual quantities, V , F are the volume and the surface of the bar, respectively, at the initial configuration and t_x , t_y , t_z are the components of the traction vector with respect to the undeformed surface of the bar. In this framework, the stress resultants are naturally defined as

$$SN = \int_{\Omega} S_{xx} d\Omega \quad SM_t^N = \int_{\Omega} S_{xx} (y^2 + z^2) d\Omega \quad (11a,b)$$

$$SM_w = \int_{\Omega} (S_{xx}\phi_S^P) d\Omega \quad SM_t^P = \int_{\Omega} \left[S_{xy} \left(\frac{\partial\phi_S^P}{\partial y} - z \right) + S_{xz} \left(\frac{\partial\phi_S^P}{\partial z} + y \right) \right] d\Omega \quad (11c,d)$$

$$SM_t^S = \frac{I_t^S}{C_S} \int_{\Omega} \left(S_{xy} \frac{\partial\phi_S^S}{\partial y} + S_{xz} \frac{\partial\phi_S^S}{\partial z} \right) d\Omega \quad (11e)$$

where SN , SM_w , SM_t^P and SM_t^S correspond to axial stress resultant, warping moment, primary and secondary twisting moments, respectively, while SM_t^N is a higher order stress resultant. It is worth here noting that these stress resultants refer to the directions of the infinitesimal elements of the cross section at its deformed configuration, since they have been defined with respect to the second Piola-Kirchhoff stress tensor [12]. Employing Equations (4) and the integrated version of Equations (8), the above stress resultants are expressed as

$$SN = EAu'_m + \frac{1}{2}EI_P(\theta'_x)^2 + SN^{pl} \quad (12a)$$

$$SM_t^N = EI_Pu'_m + \frac{1}{2}EI_{PP}(\theta'_x)^2 + SM_t^{Npl} \quad (12b)$$

$$SM_w = EC_S(\theta_x^P)'' + SM_w^{pl} \quad SM_t^P = GI_t^P\theta'_x + SM_t^{Ppl} \quad (12c,d)$$

$$SM_t^S = -GI_t^S \left((\theta_x^P)' - \theta'_x \right) + SM_t^{Spl} \quad (12e)$$

where A , I_P , I_{PP} , C_S , I_t^P , I_t^S are the area, polar moment of inertia, fourth moment of inertia, warping constant, primary (St. Venant) and secondary torsion constants of the cross section, respectively, given as [9-10]

$$A = \int_{\Omega} d\Omega \quad I_P = \int_{\Omega} (y^2 + z^2) d\Omega \quad I_{PP} = \int_{\Omega} (y^2 + z^2)^2 d\Omega \quad (13a,b,c)$$

$$C_S = \int_{\Omega} (\phi_S^P)^2 d\Omega \quad I_t^P = \int_{\Omega} \left(y^2 + z^2 + y \frac{\partial \phi_S^P}{\partial z} - z \frac{\partial \phi_S^P}{\partial y} \right) d\Omega \quad (13d,e)$$

$$I_t^S = k_x \int_{\Omega} \left[\left(\frac{\partial \phi_S^P}{\partial y} \right)^2 + \left(\frac{\partial \phi_S^P}{\partial z} \right)^2 \right] d\Omega \quad (13f)$$

while SN^{pl} , SM_t^{Npl} , SM_w^{pl} , SM_t^{Ppl} , SM_t^{Spl} are the plastic parts of the corresponding stress resultants defined as

$$SN^{pl} = -E \int_{\Omega} \varepsilon_{xx}^{pl} d\Omega \quad SM_t^{Npl} = -E \int_{\Omega} \varepsilon_{xx}^{pl} (y^2 + z^2) d\Omega \quad (14a,b)$$

$$SM_w^{pl} = -E \int_{\Omega} (\varepsilon_{xx}^{pl} \phi_S^P) d\Omega \quad (14c)$$

$$SM_t^{Ppl} = -G \int_{\Omega} \left[\gamma_{xy}^{pl} \left(\frac{\partial \phi_S^P}{\partial y} - z \right) + \gamma_{xz}^{pl} \left(\frac{\partial \phi_S^P}{\partial z} + y \right) \right] d\Omega \quad (14d)$$

$$SM_t^{Spl} = -G \frac{I_t^S}{C_S} \int_{\Omega} \left(\gamma_{xy}^{pl} \frac{\partial \phi_S^S}{\partial y} + \gamma_{xz}^{pl} \frac{\partial \phi_S^S}{\partial z} \right) d\Omega \quad (14e)$$

After substituting Equations (11) into Equation (10) and conducting some algebraic manipulations, the global equilibrium equations of the bar are obtained as

$$\frac{dSN}{dx} = -n(x) \quad (15a)$$

$$\frac{dSM_t^N}{dx} \theta'_x + SM_t^N \theta''_x + \frac{dSM_t^P}{dx} + \frac{dSM_t^S}{dx} = -m_t \quad \frac{dSM_w}{dx} + SM_t^S = m_w \quad (15b,c)$$

along with their corresponding boundary conditions

$$\alpha_1 SN + \alpha_2 u_m = \alpha_3 \quad \beta_1 SM_t^{tot} + \beta_2 \theta_x = \beta_3 \quad \bar{\beta}_1 SM_w + \bar{\beta}_2 (\theta'_x)^P = \bar{\beta}_3 \quad (16a,b,c)$$

where $SM_t^{tot} = SM_t^N \theta'_x + SM_t^P + SM_t^S$ is the total twisting moment at the bar ends, while α_i , β_i ($i = 1, 2, 3$) are functions specified at the bar ends. The boundary conditions (16) are the most general ones for the problem at hand, including also the elastic support. It is apparent that all types of the conventional boundary conditions (clamped, simply supported, free or guided edge) may be derived from Equations (16) by specifying appropriately the functions α_i , β_i and $\bar{\beta}_i$ (e.g. for a clamped

edge it is $a_2 = \beta_2 = \bar{\beta}_2 = 1$, $a_1 = a_3 = \beta_1 = \beta_3 = \bar{\beta}_1 = \bar{\beta}_3 = 0$. Moreover, the expressions of the externally applied loading (n , m_t , m_w) with respect to the components of the traction vector are resolved by virtue of Equation (10) and are presented in [10].

Employing Equations (12) and a one dimensional independent warping parameter η_x which is set equal to the primary angle of twist per unit length, the governing differential equations of the bar (Equations (15)) are expressed as

$$EAu_m'' + EI_P\theta_x'\theta_x'' + \frac{dSN^{pl}}{dx} = -n(x) \quad (17a)$$

$$G(I_t^P + I_t^S)\theta_x'' - GI_t^S\eta_x' + \frac{3}{2}EI_{PP}(\theta_x')^2\theta_x'' + EI_Pu_m'\theta_x'' + EI_Pu_m''\theta_x' + \frac{dSM_t^{Npl}}{dx}\theta_x' + SM_t^{Npl}\theta_x'' + \frac{dSM_t^{Ppl}}{dx} + \frac{dSM_t^{Spl}}{dx} = -m_t(x) \quad (17b)$$

$$EC_S\eta_x'' - GI_t^S(\eta_x - \theta_x') + \frac{dSM_w^{pl}}{dx} + SM_t^{Spl} = m_w(x) \quad (17c)$$

while Equation (16c) is also modified accordingly. Dropping the plastic quantities of the above equations, the boundary value problem of the examined problem under elastic conditions is formulated.

3 Numerical solution

3.1 Integral representations for the “average” axial displacement u_m , the angle of twist θ_x and the warping parameter η_x

According to the precedent analysis, the nonlinear inelastic nonuniform torsional problem of bars taking into account STMDE reduces to establishing the displacement components $u_m(x)$, $\theta_x(x)$, $\eta_x(x)$ having continuous derivatives up to the second order with respect to x and satisfying the boundary value problem described by the coupled governing differential equations (17) along the bar and the boundary conditions (16) at the bar ends $x=0, l$. This boundary value problem is solved employing the BEM [13], as this is developed in [9] for the solution of a system of two coupled second order differential equations, after modifying it as follows. The motivation to use this particular technique is justified from the intention to retain the advantages of a BEM solution over a domain approach, while using simple fundamental solutions and avoiding finite differences to the solution of the problem.

According to this method, let $u_1(x) = u_m(x)$, $u_2(x) = \theta_x(x)$, $u_3(x) = \eta_x(x)$ be the sought solution of the problem. The solution of the second order differential

equations $d^2u_1/dx^2 = u_m''$, $d^2u_2/dx^2 = \theta_x''$, $d^2u_3/dx^2 = \eta_x''$ are given in integral form as [9]

$$u_n(\xi) = \int_0^l \frac{d^2u_n}{dx^2} u^* dx - \left[u^* \frac{du_n}{dx} - \frac{\partial u^*}{\partial x} u_n \right]_0^l \quad (n = 1, 2, 3) \quad (18a,b,c)$$

where u^* is the fundamental solution given as $u^* = (l/2)|r|$ [9], with $r = x - \xi$, x, ξ points of the bar. Since EA , $G(I_t^P + I_t^S)$ and EC_S are independent of x , Equations (18) can be written as

$$EAu_1(\xi) = \int_0^l EA \frac{d^2u_1}{dx^2} \Lambda_2 dx - EA \left[\Lambda_2 \frac{du_1}{dx} - \Lambda_1 u_1 \right]_0^l \quad (19a)$$

$$G(I_t^P + I_t^S)u_2(\xi) = \int_0^l G(I_t^P + I_t^S) \frac{d^2u_2}{dx^2} \Lambda_2 dx - G(I_t^P + I_t^S) \left[\Lambda_2 \frac{du_2}{dx} - \Lambda_1 u_2 \right]_0^l \quad (19b)$$

$$EC_S u_3(\xi) = \int_0^l EC_S \frac{d^2u_3}{dx^2} \Lambda_2 dx - EC_S \left[\Lambda_2 \frac{du_3}{dx} - \Lambda_1 u_3 \right]_0^l \quad (19c)$$

where the kernels $\Lambda_j(r) = \Lambda_j(x, \xi)$ ($j = 1, 2$) are given as $\Lambda_1(r) = (l/2)\text{sgn}r$, $\Lambda_2(r) = (l/2)|r|$. Solving Equation (17a) with respect to EAu_m'' and substituting the result in Equation (19a), Equation (17b) with respect to $G(I_t^P + I_t^S)\theta_x''$ and substituting the result in Equation (19b) and Equation (17c) with respect to $EC_S\eta_x''$ and substituting the result in Equation (19c), the following integral representations are obtained

$$EAu_1(\xi) = \int_0^l \left(-n(x) - \frac{dSN^{pl}}{dx} - EI_P \frac{du_2}{dx} \frac{d^2u_2}{dx^2} \right) \Lambda_2 dx - EA \left[\Lambda_2 \frac{du_1}{dx} - \Lambda_1 u_1 \right]_0^l \quad (20a)$$

$$\begin{aligned} G(I_t^P + I_t^S)u_2(\xi) = & \int_0^l \left(GI_t^S \frac{du_3}{dx} - \frac{3}{2} EI_{PP} \left(\frac{du_2}{dx} \right)^2 \frac{d^2u_2}{dx^2} - EI_P \frac{du_1}{dx} \frac{d^2u_2}{dx^2} \right. \\ & - EI_P \frac{d^2u_1}{dx^2} \frac{du_2}{dx} - m_t - \frac{dSM_t^{Npl}}{dx} \frac{du_2}{dx} - SM_t^{Npl} \frac{d^2u_2}{dx^2} - \frac{dSM_t^{Ppl}}{dx} \\ & \left. - \frac{dSM_t^{Spl}}{dx} \right) \Lambda_2 dx - G(I_t^P + I_t^S) \left[\Lambda_2 \frac{du_2}{dx} - \Lambda_1 u_2 \right]_0^l \quad (20b) \end{aligned}$$

$$\begin{aligned}
EC_S u_3(\xi) = & \int_0^l \left(GI_t^S \left(u_3 - \frac{du_2}{dx} \right) + m_w - \frac{dSM_w^{pl}}{dx} - SM_t^{Spl} \right) \Lambda_2 dx \\
& - EC_S \left[\Lambda_2 \frac{du_3}{dx} - \Lambda_1 u_3 \right]_0^l
\end{aligned} \tag{20c}$$

After carrying out several integrations by parts, Equations (20) yield

$$\begin{aligned}
EAu_1(\xi) = & - \int_0^l n(x) \Lambda_2 dx + \int_0^l \frac{1}{2} EI_P \left(\frac{du_2}{dx} \right)^2 \Lambda_1 dx + \int_0^l SN^{pl} \Lambda_1 dx \\
& - \left[\left(SN^{pl} + \frac{1}{2} EI_P \left(\frac{du_2}{dx} \right)^2 \right) \Lambda_2 \right]_0^l - EA \left[\Lambda_2 \frac{du_1}{dx} - \Lambda_1 u_1 \right]_0^l
\end{aligned} \tag{21a}$$

$$\begin{aligned}
G(I_t^P + I_t^S)u_2(\xi) = & - \int_0^l m_t \Lambda_2 dx - \int_0^l \left(GI_t^S u_3 - \frac{1}{2} EI_{PP} \left(\frac{du_2}{dx} \right)^3 - EI_P \frac{du_1}{dx} \frac{du_2}{dx} \right) \Lambda_1 dx \\
& + \left[\left(GI_t^S u_3 - \frac{1}{2} EI_{PP} \left(\frac{du_2}{dx} \right)^3 - EI_P \frac{du_1}{dx} \frac{du_2}{dx} \right) \Lambda_2 \right]_0^l + \int_0^l \left(SM_t^{Npl} \frac{du_2}{dx} \right) \Lambda_1 dx \\
& - \left[\left(SM_t^{Npl} \frac{du_2}{dx} \right) \Lambda_2 \right]_0^l + \int_0^l \left(SM_t^{Ppl} + SM_t^{Spl} \right) \Lambda_1 dx - \left[\left(SM_t^{Ppl} + SM_t^{Spl} \right) \Lambda_2 \right]_0^l \\
& - G(I_t^P + I_t^S) \left[\Lambda_2 \frac{du_2}{dx} - \Lambda_1 u_2 \right]_0^l
\end{aligned} \tag{21b}$$

$$\begin{aligned}
EC_S u_3(\xi) = & \int_0^l m_w \Lambda_2 dx + \int_0^l GI_t^S \left(u_3 - \frac{du_2}{dx} \right) \Lambda_2 dx \\
& + \int_0^l SM_w^{pl} \Lambda_1 dx - \left[SM_w^{pl} \Lambda_2 \right]_0^l - \int_0^l SM_t^{Spl} \Lambda_2 dx - EC_S \left[\Lambda_2 \frac{du_3}{dx} - \Lambda_1 u_3 \right]_0^l
\end{aligned} \tag{21c}$$

The boundary terms in the above equations are more conveniently assembled as

$$\begin{aligned}
EAu_1(\xi) = & - \int_0^l n(x) \Lambda_2 dx + \int_0^l \frac{1}{2} EI_P \left(\frac{du_2}{dx} \right)^2 \Lambda_1 dx + \int_0^l SN^{pl} \Lambda_1 dx \\
& - \left[\Lambda_2 SN - \Lambda_1 EAu_1 \right]_0^l
\end{aligned} \tag{22a}$$

$$\begin{aligned}
G(I_t^P + I_t^S)u_2(\xi) &= -\int_0^l m_t A_2 dx \\
&- \int_0^l \left(GI_t^S u_3 - \frac{l}{2} EI_{PP} \left(\frac{du_2}{dx} \right)^3 - EI_P \frac{du_1}{dx} \frac{du_2}{dx} \right) A_1 dx \\
&+ \int_0^l \left(SM_t^{Npl} \frac{du_2}{dx} + SM_t^{Ppl} + SM_t^{Spl} \right) A_1 dx - \left[A_2 SM_t^{tot} - A_1 G(I_t^P + I_t^S) u_2 \right]_0^l
\end{aligned} \tag{22b}$$

$$\begin{aligned}
EC_S u_3(\xi) &= \int_0^l m_w A_2 dx + \int_0^l GI_t^S \left(u_3 - \frac{du_2}{dx} \right) A_2 dx \\
&+ \int_0^l SM_w^{pl} A_1 dx - \int_0^l SM_t^{Spl} A_2 dx - \left[A_2 SM_w - EC_S A_1 u_3 \right]_0^l
\end{aligned} \tag{22c}$$

after taking into account the expressions of Equations (12).

If secondary torsional moment deformation effects are negligible, then $u_3 \approx u_2'$. In such cases, shear locking effects could occur [12] if proper care is not undertaken. In the present numerical technique, these effects are alleviated by employing the same order of approximation for u_3 and u_2' . In order to achieve explicit appearance of u_2' in Equation (22b), this integral representation is differentiated with respect to ξ , yielding

$$\begin{aligned}
G(I_t^P + I_t^S)u_2'(\xi) &= \int_0^l m_t A_1 dx + GI_t^S u_3(\xi) - \frac{l}{2} EI_{PP} [u_2'(\xi)]^3 - EI_P u_1'(\xi) u_2'(\xi) \\
&- SM_t^{Npl} u_2'(\xi) - SM_t^{Ppl} - SM_t^{Spl} + \left[A_1 SM_t^{tot} \right]_0^l
\end{aligned} \tag{23}$$

Moreover, observing Equations (4) it is deduced that u_1' , u_3' must also be computed in order to resolve the strain components (as well as the plastic parts of stress resultants), thus the integral representations (22a,c) are differentiated with respect to ξ , yielding

$$EAu_1'(\xi) = \int_0^l n(x) A_1 dx - \frac{l}{2} EI_P [u_2'(\xi)]^2 - SN^{pl}(\xi) + \left[A_1 SN \right]_0^l \tag{24a}$$

$$\begin{aligned}
EC_S u_3'(\xi) &= -\int_0^l m_w A_1 dx - \int_0^l GI_t^S \left(u_3 - \frac{du_2}{dx} \right) A_1 dx - SM_w^{pl}(\xi) \\
&+ \int_0^l SM_t^{Spl} A_1 dx + \left[A_1 SM_w \right]_0^l
\end{aligned} \tag{24b}$$

In order to alleviate potential membrane locking effects [12], the integral representation (22b) is reformulated exploiting Equation (24a) as

$$\begin{aligned}
G(I_t^P + I_t^S)u_2(\xi) = & -\int_0^l m_t \Lambda_2 dx - \int_0^l \left(GI_t^S u_3 - \frac{I}{2} EI_n \left(\frac{du_2}{dx} \right)^3 \right) \Lambda_I dx \\
& + \frac{I_P}{A} \int_0^l \left(\frac{du_2}{dx} \int_0^l n(t) \Lambda_I(t, x) dt \right) \Lambda_I(x, \xi) dx + \frac{I_P}{2A} (SN(0) + SN(l)) \int_0^l \frac{du_2}{dx} \Lambda_I dx \\
& + \int_0^l \left(\left(SM_t^{Npl} - \frac{I_P}{A} SN^{pl} \right) \frac{du_2}{dx} + SM_t^{Ppl} + SM_t^{Spl} \right) \Lambda_I dx \\
& - \left[\Lambda_2 SM_t^{tot} - \Lambda_I G(I_t^P + I_t^S) u_2 \right]_0^l
\end{aligned} \tag{25}$$

where I_n is a geometric constant defined as $I_n = I_{PP} - (I_P)^2 / A$.

Noting that the plastic parts of the stress resultants depend on u'_1 , u'_2 , u_3 , u'_3 , it is deduced that Equations (22c), (23-24) have been brought into a convenient form to establish a numerical solution of the problem at hand. Thus, the interval $(0, l)$ is divided into L elements, on each of which u_3 , u'_2 and the plastic parts of the stress resultants (Equations (14)) are assumed to vary according to a certain law (constant, linear, parabolic etc). The linear element assumption is employed here (Figure 2) as the numerical implementation is simple and the obtained results very good. This technique avoids differentiation of shape functions and does not require any finite differences. Employing a collocation technique, a set of $4L + 4$ algebraic equations is obtained with respect to $4L + 10$ unknowns, namely the values of $(u'_1)_i$, $(u'_2)_i$, $(u_3)_i$, $(u'_3)_i$ ($i = 2, 3, \dots, L$) at the $L - 1$ internal nodal points and the boundary values of $(u'_1)_j$, $(u'_2)_j$, $(u_3)_j$, $(u'_3)_j$, $(SN)_j$, $(SM_t^{tot})_j$, $(SM_w)_j$ ($j = 1, L + 1$) at the bar ends $\xi_1 = 0$, $\xi_{L+1} = l$ (Figure 2)). Four additional algebraic equations are obtained by applying the integral representations (22a), (25) at the bar ends $\xi = 0, l$ along with four additional unknowns, namely the boundary values of $(u_1)_j$, $(u_2)_j$ ($j = 1, L + 1$). These $4L + 8$ equations along with the six boundary conditions (Equations (16)) yield a system of $4L + 14$ simultaneous nonlinear algebraic equations

$$\left[K(\{d\}) \right] \{d\} = \{b_{ext}\} + \{b_{pl}(\{d\})\} \tag{26}$$

where $[K]$ is a generalized elastic (geometrically) nonlinear stiffness matrix, $\{d\}$ is a generalized unknown vector given as

$$\begin{aligned}
\{d\}^T = & \{(u'_1)_2 \ (u'_1)_3 \ \dots \ (u'_1)_L \ (u'_2)_2 \ (u'_2)_3 \ \dots \ (u'_2)_L \\
& (u_3)_2 \ (u_3)_3 \ \dots \ (u_3)_L \ (u'_3)_2 \ (u'_3)_3 \ \dots \ (u'_3)_L \\
& (u_1)_1 \ (u_1)_{L+1} \ (u'_1)_1 \ (u'_1)_{L+1} \ (u_2)_1 \ (u_2)_{L+1} \ (u'_2)_1 \ (u'_2)_{L+1} \ (27) \\
& (u_3)_1 \ (u_3)_{L+1} \ (u'_3)_1 \ (u'_3)_{L+1} \ (u_2)_1 \ (u_2)_{L+1} \\
& \left. \left(\Delta SM_t^{tot} \right)_1 \ \left(\Delta SM_t^{tot} \right)_{L+1} \ (\Delta SM_w)_1 \ (\Delta SM_w)_{L+1} \right\}
\end{aligned}$$

while $\{b_{ext}\}$, $\{b_{pl}\}$ are vectors representing all the terms related to the externally applied loading and the plastic parts of the stress resultants, respectively. Finally, after solving the system of Equations (26) the kinematical components $u_1(x) = u_m(x)$, $u_2(x) = \theta_x(x)$ at any interior point of the bar may be computed by employing Equations (22a) and (25), respectively.

3.2 Integral representations for the primary ϕ_S^P and secondary ϕ_S^S warping functions and geometric constants $A, I_P, I_{PP}, C_S, I_t^P, I_t^S, k_x$

The evaluation of the primary warping function ϕ_S^P and of its derivatives with respect to y and z at any interior point is accomplished using BEM as this is outlined in [2]. The evaluation of the secondary warping function ϕ_S^S (and of its derivatives with respect to y and z) is accomplished using BEM [2]. The evaluation of A , I_P , I_{PP} and of C_S , I_t^P , I_t^S (once ϕ_S^P is established) is performed through line integrals along the boundary of the cross section [2, 14, 9]. Finally, once ϕ_S^S is established, the evaluation of k_x is performed through a domain integral along the cross section [9].

3.3 Incremental - iterative solution algorithm

In the present study, external loading is considered at a number of stations which are chosen according to load history and convergence requirements. Load control over the incremental steps is employed. At each load station, the system of nonlinear equations (26) is numerically solved employing an iterative solution strategy which is a modification of Powell's hybrid algorithm [15]. This algorithm is a variation of Newton's method [15] requiring the following quantities.

- i. A Jacobian matrix of the system of nonlinear equations which corresponds to a generalized stiffness matrix to the problem at hand. In this study, this matrix is approximated with finite differences [15] avoiding in this manner its explicit derivation.

- ii. An initial guess of the solution $\{d_{init}\}$ (at each load station). The resolved vector $\{d\}$ of the previously converged load station is employed in this study ($\{d\} = \{0\}$ is used at the first load station).
- iii. A tolerance parameter tol_{gl} to perform the stopping criterion of the algorithm. Values $tol_{gl} = 10^{-5} \div 10^{-7}$ have been used in this study.

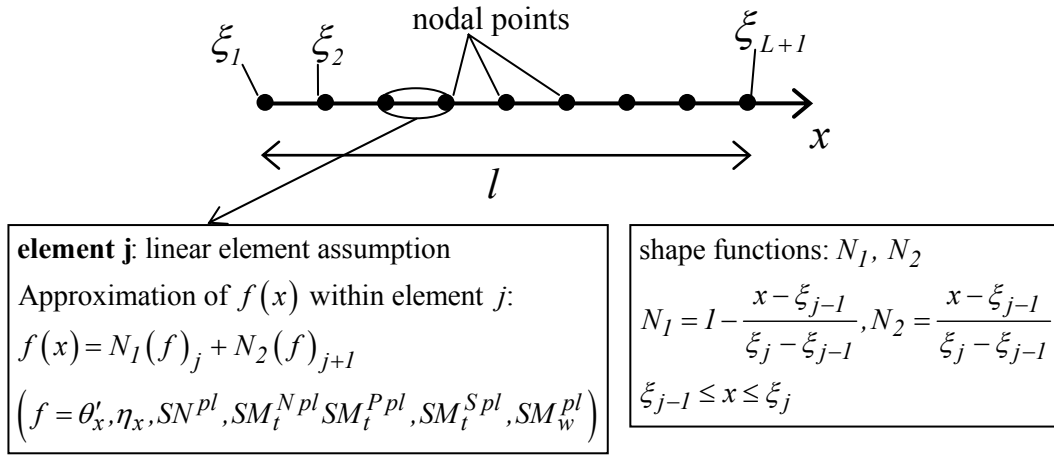


Figure 2: Discretization of the bar interval into linear elements, distribution of the nodal points and approximation of several quantities.

A number of monitoring cross sections is defined coinciding with the $L + 1$ nodal points of the bar interval (Figure 2). These sections are divided into a number of triangular or quadrilateral cells and standard two-dimensional Gauss quadrature rules are employed in each cell to resolve the plastic parts of the stress resultants (Equations (14)). Thus, the monitoring stations of each cross section coincide with the Gauss points of its cells, while exact patch between adjacent cells is not required [9].

At each load station, the system of nonlinear equations (26) is expressed without explicitly deriving its incremental form which is lengthier due to terms associated with geometrical nonlinearity. This is achieved by exploiting values of $S_{xx}, S_{xy}, S_{xz}, u'_m, \theta'_x, \eta_x, \eta'_x, \varepsilon_{eq}^{pl}, \varepsilon_{xx}^{pl}, \gamma_{xy}^{pl}, \gamma_{xz}^{pl}$ of the previously converged load station at the monitoring stations of the bar and adhering to the following steps (subscript *cur* denotes the current value of a quantity that is iteratively updated through the algorithm and subscript *conv* denotes the converged value of a quantity at a previous load station).

- i. At each monitoring station of the bar, evaluate the trial stress components as

$$S_{xx}^{Tr} = (S_{xx})_{conv} + E \left((u'_m)_{cur} - (u'_m)_{conv} \right) + E \left((\eta'_x)_{cur} - (\eta'_x)_{conv} \right) \phi_S^P + E \frac{I}{2} (y^2 + z^2) \left((\theta'_x)_{cur}^2 - (\theta'_x)_{conv}^2 \right) \quad (28a)$$

$$S_{xy}^{Tr} = (S_{xy}^{Tr})_{conv} + G \left((\theta'_x)_{cur} - (\theta'_x)_{conv} \right) \left(\frac{\partial \phi_S^P}{\partial y} - z \right) - G \left[(\eta_x)_{cur} - (\theta'_x)_{cur} - \left((\eta_x)_{conv} - (\theta'_x)_{conv} \right) \right] \frac{I_t^S}{C_S} \left(\frac{\partial \phi_S^S}{\partial y} \right) \quad (28b)$$

$$S_{xz}^{Tr} = (S_{xz}^{Tr})_{conv} + G \left((\theta'_x)_{cur} - (\theta'_x)_{conv} \right) \left(\frac{\partial \phi_S^P}{\partial z} + y \right) - G \left[(\eta_x)_{cur} - (\theta'_x)_{cur} - \left((\eta_x)_{conv} - (\theta'_x)_{conv} \right) \right] \frac{I_t^S}{C_S} \left(\frac{\partial \phi_S^S}{\partial z} \right) \quad (28c)$$

ii. At each monitoring station of the bar, perform the yield criterion employing Equation (9).

- If $f^{Tr} = \sqrt{(S_{xx}^{Tr})^2 + 3 \left((S_{xy}^{Tr})^2 + (S_{xz}^{Tr})^2 \right)} - \sigma_Y \left((\varepsilon_{eq}^{pl})_{conv} \right) \leq 0$ then the trial state is the final state, the incremental plastic strain components are zero and the total plastic strain components along with the equivalent plastic strain get the corresponding values of the previously converged load station.
- If $f^{Tr} > 0$ then plastic flow occurs and return must be made to yield surface (plastic correction step). A local Newton – Raphson method is initiated to integrate the inelastic constitutive equations by employing the generalized cutting-plane algorithm [16]. The incremental plastic strain components along with the equivalent plastic strain are updated according to this algorithm by using a prescribed tolerance $tol = 10^{-5}$ in its convergence criterion and subsequently the total plastic strain components are resolved by adding the corresponding incremental quantities to the ones of the previously converged load station.

iii. At each monitoring cross section of the bar, evaluate numerically the plastic parts of the stress resultants (Equations (14)).

iv. Employ the obtained plastic parts of the stress resultants to evaluate the vector $\{b_{pl}\}_{cur}$ of Equation (26). Apart from elementary computations, this step requires the computation of line integrals along the bar interval which is performed employing a semi-analytical scheme [9]. It is worth noting here that the line integrals arising in the term $[K]_{cur} \{d\}_{cur}$ of Equation (26) (including the ones associated with geometrical nonlinearity) are also computed semi-analytically without any special difficulty.

Finally, it is worth noting that the monitoring displacement components θ_x , η_x at any interior point of the bar are updated after convergence in each increment by employing Equations (22a), (25), respectively.

4 Numerical examples

4.1 Example 1

In the first example, for comparison reasons, an elastic bar of narrow rectangular cross section $10 \times 200 \text{ mm}$ ($E = 2.0 \times 10^8 \text{ kN/m}^2$, $G = 8.0 \times 10^7 \text{ kN/m}^2$) of length $l = 1.0 \text{ m}$, subjected to a uniformly distributed torque per unit length m_t has been studied, employing 50 longitudinal elements, 300 boundary elements, 64 quadrilateral cells and a 2×2 Gauss integration scheme for each cell (cross sectional discretization). The bar's ends are simply supported according to its torsional boundary conditions, while the left end is immovable and the right end is free to move according to its axial boundary conditions. In Figure 3 the variation of the angle of twist θ_x at the midspan with respect to the applied external torque per unit length m_t is presented as compared with the values obtained from a BEM-based [17] and a FEM solution [18] which both ignore the STMDE. Excellent agreement is achieved with the existing studies, verifying the proposed numerical procedure at the elastic geometrically nonlinear regime. It is also concluded that geometrical nonlinearity increases the torsional rigidity of the bar, while the STMDE influences negligibly nonlinear elastic torsional analysis of open thin-walled cross section bars.

4.2 Example 2

In the second example, for comparison reasons an open thin-walled I-shaped (total height $h = 0.1524 \text{ m}$, total width $b = 0.1509 \text{ m}$, flange width $t_f = 0.0122 \text{ m}$, web width $t_w = 0.0080 \text{ m}$) cross section bar ($E = 213400 \text{ MN/m}^2$, $G = 80000 \text{ MN/m}^2$, $\sigma_{Y0} = 285 \text{ MN/m}^2$, $E_t = 0 \text{ MN/m}^2$) of length $l = 1.93 \text{ m}$ subjected to a monotonically increasing concentrated twisting moment at its midpoint and restrained against twisting at both ends (free warping boundary conditions) has been studied, employing 36 longitudinal elements, 500 boundary elements, 64 quadrilateral cells and a 3×3 Gauss integration scheme for each cell (cross sectional discretization). Two cases of axial boundary conditions have been studied, namely case A in which both ends are axially immovable and case B in which the left end is immovable and the right end is free to move. In Figure 4, the corresponding torque - angle of twist curves at the midpoint of the bar are presented as compared with a FEM solution [7] that ignores the STMDE and experimental results [19]. From this figure, very good agreement between the results of the proposed method and those of the existing studies is observed. It is also concluded that large twisting rotations

affect significantly the behavior of the bar since it is not led to plastic collapse, while the STMDE influences negligibly nonlinear inelastic torsional analysis of open thin-walled cross section bars. Finally, it is remarked that axial restraints at the bar ends increase further the torsional rigidity of the bar, especially at larger twisting rotations.

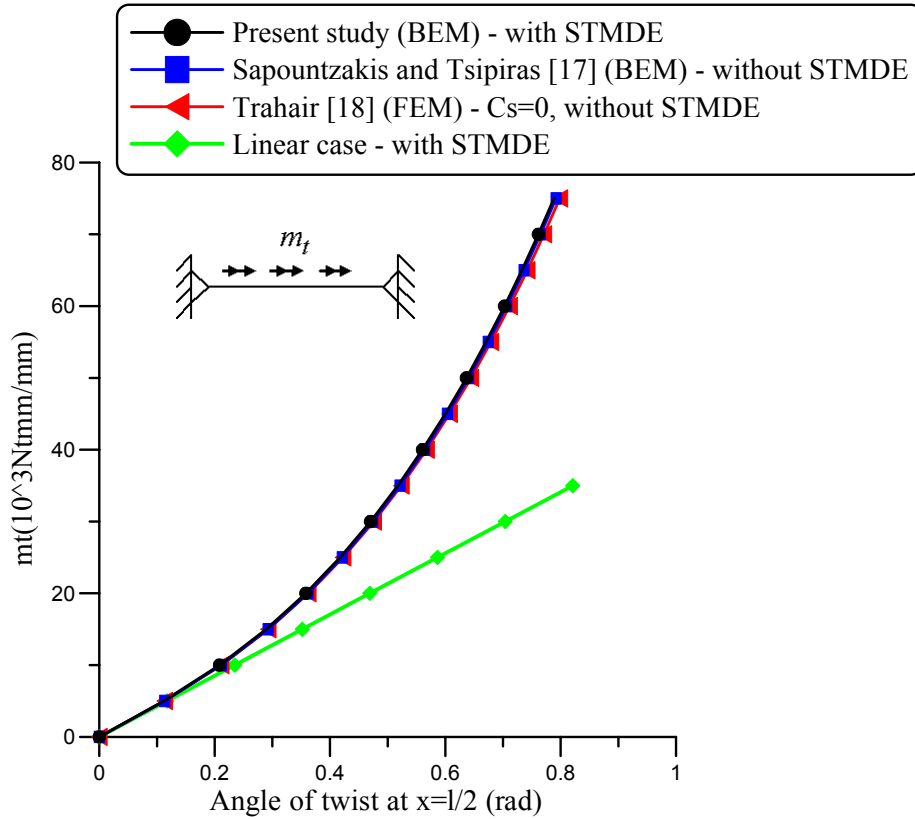


Figure 3: Torque - angle of twist curves at $x = l/2$ of the bar of example 1.

5 Concluding remarks

The main conclusions that can be drawn from this investigation are:

- Large twisting rotations increase the torsional rigidity of bars. This effect is more pronounced in presence of axial restraints at the bar ends.
- STMD effect is negligible in nonlinear torsional analysis of open thin-walled cross section bars.
- Explicit derivation of the incremental form of the discretized global equilibrium equations is not required in the developed methodology.
- Finite differences and differentiation of shape functions are not required in the discretization of the global equilibrium equations.
- The procedure developed retains most of the advantages of a BEM solution over a domain approach.

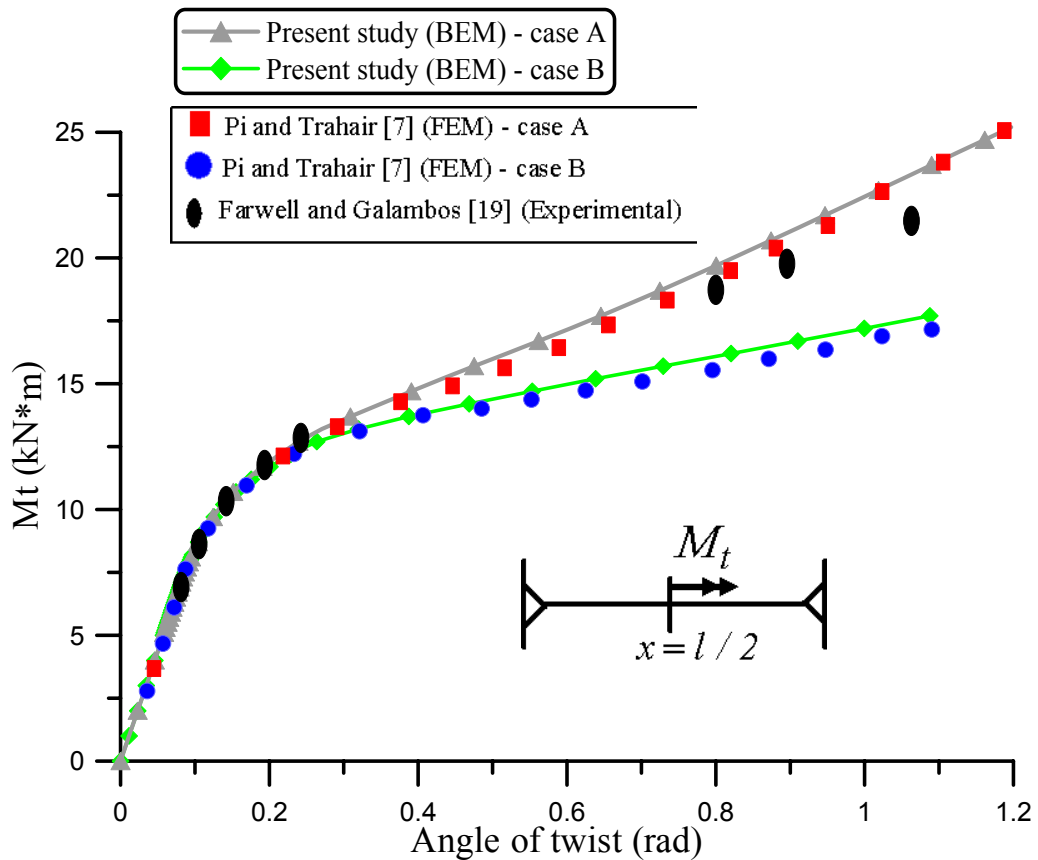


Figure 4: Torque - angle of twist curves at $x = l/2$ of the bar of example 2.

References

- [1] P. Nukala, D. White, "A mixed finite element for three-dimensional nonlinear analysis of steel frames", *Computer Methods in Applied Mechanics and Engineering*, 193, 2507-2545, 2004.
- [2] E.J. Sapountzakis, V.G. Mocos, "Warping shear stresses in nonuniform torsion by BEM", *Computational Mechanics*, 30, 131-142, 2003.
- [3] H. Rubin, "Wölbkrafttorsion von Durchlaufträgern Mit Konstantem Querschnitt Unter Berücksichtigung Sekundärer Schubverformungen", *Stahlbau*, 74, 826-842, 2005.
- [4] V.G. Mocos, E.J. Sapountzakis, "Secondary torsional moment deformation effect by BEM", *International Journal of Mechanical Sciences*, 53, 897-909, 2011.
- [5] M.M. Attard, "Nonlinear theory of non-uniform torsion of thin-walled open beams", *Thin-Walled Structures*, 4, 101-134, 1986.
- [6] F. Gruttmann, R. Sauer, W. Wagner, "Theory and numerics of three-dimensional beams with elastoplastic material behaviour", *International Journal for Numerical Methods in Engineering*, 48, 1675-1702, 2000.

- [7] Y.L. Pi, N.S. Trahair, “Inelastic torsion of steel I-beams” *Journal of Structural Engineering*, ASCE, 121(4), 609-620, 1995.
- [8] E.J. Sapountzakis, V.J. Tsipiras, “Inelastic Nonuniform Torsion of Bars of Doubly Symmetric Cross Section by BEM”, *Computers and Structures*, 89, 2388-2401, 2010.
- [9] V.J. Tsipiras, E.J. Sapountzakis, “Secondary Torsional Moment Deformation Effect in Inelastic Nonuniform Torsion of Bars of Doubly Symmetric Cross Section by BEM”, *International Journal of Non-Linear Mechanics*, 47, 68-84, 2012.
- [10] E.J. Sapountzakis, V.J. Tsipiras, “Shear Deformable Bars of Doubly Symmetrical Cross Section Under Nonlinear Nonuniform Torsional Vibrations – Application to Torsional Postbuckling Configurations and Primary Resonance Excitations”, *Nonlinear Dynamics*, 62, 967-987, 2010.
- [11] D.O. Brush, B.O. Almroth, “Buckling of bars, plates and shells”, McGraw - Hill Book Co, New York, 1975.
- [12] M.A. Crisfield, “Non-linear Finite Element Analysis of Solids and Structures, Vol. 1: Essentials”, John Wiley and Sons, New York, USA, 1991.
- [13] J.T. Katsikadelis, “Boundary Elements: Theory and Applications”, Elsevier, Amsterdam-London, United Kingdom, 2002.
- [14] E.J. Sapountzakis, V.J. Tsipiras, “Nonlinear Nonuniform Torsional Vibrations of Bars by the Boundary Element Method”, *Journal of Sound and Vibration*, 329, 1853-1874, 2010.
- [15] IMSL, “User’s manual, IMSL MATH/Library: Fortran subroutines for mathematical applications”, Visual Numerics Inc., Houston, USA, 1997.
- [16] M. Ortiz, J.C. Simo, “An analysis of a new class of integration algorithms for elastoplastic constitutive relations”, *International Journal for Numerical Methods in Engineering*, 23, 353–366, 1986.
- [17] E.J. Sapountzakis, V.J. Tsipiras, “Non-linear Elastic Non-uniform Torsion of Bars of Arbitrary Cross-Section by BEM”, *International Journal of Non-Linear Mechanics*, 45, 63-74, 2010.
- [18] N.S. Trahair, “Nonlinear Elastic Nonuniform Torsion”, *Journal of Structural Engineering*, 131, 1135–1142, 2005.
- [19] C.R.Jr. Farwell, T.V. Galambos, “Nonuniform torsion of steel beams in inelastic range”, *Journal of Structural Engineering*, ASCE, 95, 2813-2829, 1969.